ACS Sustainable Chemistry & Engineering

Research Article

pubs.acs.org/journal/ascecg

Development of Greener Multi-Responsive Chitosan Biomaterials Doped with Biocompatible Ammonium Ionic Liquids

A. M. A. Dias,[†] A. R. Cortez,[†] M. M. Barsan,[‡] J. B. Santos,[§] C. M. A. Brett,*[,‡] and H. C. de Sousa*[,†]

[†]CIEPQPF, Chemical Engineering Department, FCTUC, University of Coimbra, Pólo II – Pinhal de Marrocos, 3030-790 Coimbra, Portugal

[‡]Chemistry Department, FCTUC, University of Coimbra, Rua Larga, 3004-535 Coimbra, Portugal

[§]Department of Electrical and Computers Engineering, University of Coimbra, 3030-290 Coimbra, Portugal

ABSTRACT: There is a current interest in the development of new stimuli-responsive materials using biodegradable and biocompatible molecules, mainly if biomedical applications are envisaged. In this work, chitosan (a cationic polyelectrolyte obtained from renewable resources) and two ammonium-based ionic liquids (ILs), namely, choline chloride ([Ch][Cl]) and choline dihydrogen phosphate ([Ch][DHP]), were used to develop biocompatible and biodegradable materials that can be used as improved electrical and pH-sensitive drug delivery systems. The influence of each IL and of residual acetic acid on the properties of chitosan-based films was evaluated. Results showed that the employed ILs can affect the water vapor sorption capacities, water vapor transmission rates, elastic moduli, and impedances/conductivities of chitosan films. Acidic pH conditions significantly enhanced the conductivity and the actuation capacity of the films, and this effect was more pronounced for films loaded with [Ch][DHP]. The potential use of these films as tunable and stimuli-responsive drug delivery systems was also studied for chitosan films loaded with [Ch][DHP] and sodium phosphate dexamethasone (DXA). The amount of DXA released from films doped with [Ch][DHP] was always lower than for films without IL, independent of the pH of the release medium. Therefore, choline-based ILs can be used as additives to tune drug release profiles of ionic drugs from chitosan-based materials. Furthermore, the simultaneous effect of ILs on the conductivities/impedances of films will allow the development of biocompatible and biodegradable drug delivery responsive systems for several biomedical/pharmaceutical applications such as iontophoretic devices.

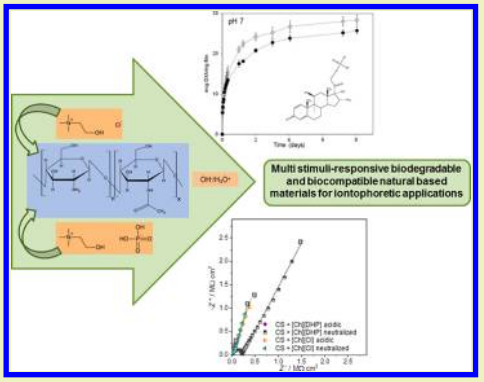

KEYWORDS: *Chitosan, Choline chloride, Choline dihydrogen phosphate, Multi-stimuli responsive biomaterials, Drug delivery, Dexamethasone*

INTRODUCTION

Stimuli-sensitive materials are defined as those that can undergo noticeable physical and/or chemical modifications in response to small changes in local environments.[1,2] Special attention has been given to macromolecular polymeric systems that are sensitive to biological changes in concentration, pH, temperature, and ionic strength.[3] However, light, electrical charge, magnetic fields, and ultrasounds can also work as efficient triggering stimuli.[4] In addition and employing appropriate and controlled design procedures, it is possible to enhance the response performances by changing polymeric conformation, solubility, degradability, and self-assembly behavior. Depending on the desired final application, other polymeric functional properties can be easily tuned (e.g., wettability, permeability, adhesion, adsorption, mechanical, and optical).[3,5] These environmentally sensitive biomaterials may present clear advantages in different pharmaceutical and biomedical applications, namely, as controlled drug delivery systems, artificial muscles/organs, scaffolds for tissue engineering, biosensors and diagnostic systems, soft-actuators, microelectrochemical systems, etc.[3,5]

Some of the most recent research in the field has been focused on the development of multiple stimuli-responsive biomaterials that can be precisely tuned to produce narrow responses for specific and well-defined external conditions. Biocompatible polyelectrolytes represent a remarkable class of stimuli-responsive biomaterials because they can respond to pH, ionic strength, and electrical current stimuli.[6] Therefore, these materials may find several promising applications for pharmaceutical and biomedical applications, namely, as controlled drug delivery systems (e.g., as the result of stimuli-induced swelling/deswelling behaviors) and as artificial muscles/organs and tissue engineering scaffolds (e.g., as the result of their ability to convert electrical information into mechanical perturbation/actuation).[7,8] Many advantages can arise from the use of electrically sensitive biopolymers, the most important being the versatility and tunable response that can be obtained simply by controlling the applied current (e.g., if it is

Received: July 27, 2013
Published: August 21, 2013

   dx.doi.org/10.1021/sc4002577 | ACS Sustainable Chem. Eng. 2013, 1, 1480–1492

continuous or pulsatile) or by controlling the duration of the electrical pulse and the period between them.[6,9]

Chitosan (CS) is an example of a versatile, abundant, and natural cationic polyelectrolyte (obtained from biorenewable sources) that has been extensively studied and used for a variety of pharmaceutical and biomedical applications. This is mostly due to its biocompatibility, nontoxicity, biodegradability, hemostatic and antimicrobial activities, mucoadhesive properties, and excellent processability (including film-forming abilities).[10−12] CS and CS-based hydrogels are also electrically responsive biomaterials. However, their low sensitivities, reversibility behaviors, conductivities, and their "soft-material" intrinsic characters usually compromise the desired functional performances after several on−off switching induced stimuli. To overcome these issues, additives such as chemical/physical cross-linkers, nanoparticles, or ionic substances (including ionic liquids) have been incorporated into CS-based hydrogels in order to improve their mechanical properties, swelling−deswelling behaviors, and conductivity/fatigue capacities. In addition, these additives will also promote significant effects on their electrical deformation and relaxation behaviors, as well as on the improvement of their stimuli-induced responsiveness.[13,14]

Ionic liquids (ILs) are organic salts, comprising a cation and an anion, which are liquids at temperatures below 100 °C. They have been presented as greener organic solvent alternatives mainly because of their good thermal stabilities, negligible vapor pressures, broad liquid ranges, tailor-made potentialities, and excellent dissolution capabilities (for organic/inorganic compounds and for natural polymers).[15−17] These properties make them suitable to be applied, for example, as plasticizers,[18] catalysts,[19] extraction solvents,[20] and for the production of advanced polymeric materials.[21] Because of their ionic nature, ILs also present a broad electrochemical window that justifies their recent use to improve the conductivity of various materials, especially polymers and polymer composites.[22−26] As examples, polymeric materials doped with ILs can be used as solid electrolytes in dye-sensitive solar cells for photovoltaic applications,[25] and as electrochemical actuators.[23,27−30]

Despite the above-mentioned advantages of using ILs, recent intensive research has been done concerning their risks and toxicity (for humans and the environment), biocompatibility, biosorption, bioaccumulation, and biodegradation pathways, principally if biomedical applications are envisaged. It was reported that the cation headgroup has the major role on the IL toxicity and that longer side chains have a more severe impact on living cells.[31] However, IL anions are responsible for some of the physico-chemical properties of these salts (e.g., lipophilicity) that can indirectly affect their toxicities. Among the different IL families, ammonium-based ILs, and more particularly choline-based ILs, are considered to be the most promising and safer ILs to be used in the development of pharmaceutical and medical applications. This is due to the fact that choline is a natural substance (it is an essential nutrient that is present in several food sources) that shows a very low toxicity and that also works as an antimicrobial and a cell signaling agent.[32,33] Choline chloride, [Ch][Cl], and choline dihydrogenphosphate, [Ch][DHP], are quaternary ammonium salts that despite being solid at room temperature are considered to be molten salts because they liquefy at high relative humidity (RH) or when mixed with small amounts of water.[34,35] [Ch][Cl] is a nontoxic, highly biocompatible, nonmutagenic, and biodegradable substance.[36] On the other hand, [Ch][DHP] has been reported as an excellent solvent for cytochrome *c*, lysozyme, and ribonuclease A, and improves the thermal stability and shelf life of several model proteins.[23,37,38] When combined with collagenous biomaterials, [Ch][DHP] exhibited excellent cell viability and adhesion properties as required for biomedical implants applications. It was also recently suggested as an alternative and less toxic cross-linker for collagen.[36] Another interesting feature of this IL is that it has a stable plastic crystalline phase over a range of almost 100 °C (between 23 and 122 °C) and in which the ionic conductivity changes from 10^{-6} to 10^{-3} S cm^{-1}. These organic plastic crystals are attractive proton-conducting materials that can be used as solid-state solvents for fuel cell electrolytes (and to replace volatile solvents).[39,40] Recently, it was reported that improved proton conductivities can be obtained by mixing [Ch][DHP] with phosphoric acid in order to prepare thermally stable electrolyte materials.[41]

This work aims to evaluate the capacity of two biocompatible ammonium-based ILs ([Ch][Cl] and [Ch][DHP]) to act as modifiers for the external stimuli responsiveness of a biocompatible/biodegradable natural polyelectrolyte hydrogels (based on chitosan). This study has two specific goals: (i) to study the influence of choline-based ILs on the impedance properties of CS films (by testing two different anions and employing acidic conditions) and (ii) to study the influence of choline-based ILs on the release profiles of an ionic drug (sodium phosphate dexamethasone, DXA). To achieve these goals, nonloaded and IL-loaded CS films were prepared and characterized in terms of their thermal stability, electrical resistivity and impedance, actuation capacity, water vapor sorption, and transmission capacity, and of their DXA-controlled release profiles. The results obtained in this work allowed the identification of the most suitable system to be further optimized for the development of improved, safer, and cheaper electrically modulated biodegradable drug release systems (namely, of chitosan-based hydrogels for iontophoretic applications).

MATERIALS AND METHODS

Materials. Chitosan (medium molecular weight) and sodium phosphate dexamethasone (DXA, 98%) were obtained from Sigma-Aldrich, Portugal. The salts used to create the controlled relative humidity (RH) conditions were potassium sulfate (90% RH at 37 °C) and lithium chloride (10% RH at 37 °C) and were also both from Sigma. The ionic liquids, choline chloride ([Ch][Cl]) or choline dihydrogenphosphate ([Ch][DHP]), with purities higher than 98% were both from Iolitec, Germany. Glacial acetic acid (99%) was from Panreac, Spain. Buffers used for the water swelling and release experiments were prepared as follows (for 500 mL of buffer solution): pH 4 (0.07 g of sodium acetate, 2.87 g of NaCl (both from Sigma-Aldrich, Portugal), and 0.23 mL of acetic acid dissolved in bidistilled water), pH 7 (0.31 g of $NaH_2PO_4.2H_2O$ and 0.52 g of $Na_2HPO_4.2H_2O$ (both from Riedel-de Haen) and 2.29 g of NaCl dissolved in bidistilled water), and pH 10 (0.23 g of $NaHCO_3$ and 0.07 g of Na_2CO_3 (both from Merck) dissolved in bidistilled water). The final pH values were precisely checked using a pH meter (Standard pH Meter, Meter Lab).

Preparation of Nonloaded and Ionic Liquid/DXA-Loaded Chitosan Films. Chitosan (CS) was dissolved in an acidic solution (1% v/v using glacial acetic acid) to a final concentration of 1% w/v and stirred overnight. The pH of the solution was adjusted to 3.5 using additional glacial acetic acid. A known volume of the CS solution (15 mL) was cast on polystyrene Petri dishes and evaporated at 50 °C for 2 days. CS films loaded with choline chloride ([Ch][Cl]) or choline dihydrogenphosphate ([Ch][DHP]) were obtained by the addition of

different amounts of each ionic liquid (25%, 50%, and 75% of the amount of CS, on a molar basis, considering the average molecular mass of CS to be equal to 145 000 g mol^{-1}) to 15 mL of the CS solution. Solutions were stirred vigorously for approximately 12 h and cast in polystyrene Petri dishes at 50 °C for 2 days. Part of the prepared films was later neutralized by immersion into 20 mL of a NaOH solution (0.5 M) for approximately 10 s and then washed three times with bi-distilled water. These films were dried for 24 h at 37 °C.

For the preparation of ionic liquid/DXA CS films, 5 mg of sodium phosphate dexamethasone (DXA) was added to 15 mL of nonloaded and 75% [Ch][DHP]-loaded CS solutions (3.3% w/w). The solutions were stirred for 24 h at room temperature and protected from light (to avoid DXA degradation). After stirring, prepared solutions were cast, dried, and neutralized as described before.

Physical Characterization of Nonloaded and of Ionic Liquid/DXA-Loaded Chitosan Films. *Morphology.* Scanning electron microscopy (SEM) (Jeol, JSM-5310, Japan) micrographs of non-neutralized and IL-loaded (75%) and nonloaded CS films were obtained at 10 kV and at different magnifications. Samples were cryo-fractured with liquid nitrogen and stored at a 20% RH and room temperature before analysis. Samples were coated with gold (approximately 300 Å) under an argon atmosphere.

Hydrophilicity. The water vapor sorption capacity of prepared films (squared 1 cm^2 samples, previously stored at 20% RH and room temperature) was measured by keeping the samples in small flasks inside a desiccator containing a potassium sulfate saturated solution to create a RH of ≈90% at 37 °C. Each system (sample + flask) was weighed before the storage at the controlled atmosphere. Each system was weighed during 8 h, at regular time intervals of 1 h. An empty flask was also used as a control. The water vapor sorption (WVS) was calculated as the ratio between the weight of water absorbed at time t (weight of the sample at time t minus the weight at $t = 0$) and the weight of the dry film (before being placed at controlled temperature/RH). The results are presented in terms of g_{water}/g_{film} and are the average of three replicates. Measurements were performed for IL-loaded (75%) and nonloaded, neutralized, and non-neutralized CS films.

Water Vapor Permeability (WVP). Film samples (with a transmission exposed area of ∼0.64 cm^2) were firmly fixed on the top of vials containing 1 mL of water. Vials were then placed into a desiccator containing lithium chloride (10% RH at 37 °C). The water vapor transferred through the tested films was determined by measuring the water weight loss (change in the weight of the vials) at regular time intervals (every hour during the first 8 h and then every 24 h) until a constant weight decrease was achieved. The slope of the water weight loss over time, under steady state conditions, was used to calculate the water vapor transmission rate (WVTR), according to the following equation

$$\mathrm{WVTR} = \frac{\Delta w}{\Delta t \times A} \quad (1)$$

where $\Delta w/\Delta t$ is the amount of water lost per unit of time (g h^{-1}) and, A is the exposed water vapor transmission area (cm^2).

The water vapor permeability was then calculated using eq 2

$$\mathrm{WVP} = \mathrm{WVTR} \times \frac{l}{P_{\mathrm{H2O}}^{37^\circ C} \times \Delta \mathrm{RH}_{\mathrm{in\text{-}out}}} \quad (2)$$

where "l" is the film thickness (mm), $P_{\mathrm{H2O}}^{37\ ^\circ C}$ is the water vapor pressure at 37 °C (6.28 kPa), and $\Delta \mathrm{RH}_{\mathrm{in-out}}$ is the relative humidity difference between the inside of the permeability cell (assumed to be 100%) and in the desiccator (assumed to be 10%). The calculated WVP, expressed in (g h^{-1} m^{-1} kPa^{-1}), resulted from the average of three replicates that were performed for each tested film. Measurements were performed for IL-loaded (75%) and nonloaded, neutralized, and non-neutralized CS films.

Water Swelling at Different pH Conditions. Squared films of 1 cm^2 were kept at 20% RH and room temperature for 24 h before swelling measurements. After initial weighing, each sample was immersed into buffer solutions at different pH (4, 7, and 10) and at fixed ionic strength (0.1 M) and into bi-distilled water (at 37 °C). After 30 min, films were taken out from the buffer solutions, weighed after removing the excess surface water with a filter paper, and placed back into the same buffer solution. This procedure was repeated at regular time intervals and up to 8 h. Water swelling (WS) was calculated as the ratio between the weight of water absorbed at time t (weight of the sample at time t minus the weight at $t = 0$) and the initial weight of the film (before immersion, $t = 0$). WS results are presented in terms of g_{water}/g_{film} and are the average of three replicates. Measurements were performed for IL-loaded (75%) and nonloaded neutralized films.

Thermo-Mechanical Properties. Thermogravimetric analyses (TGA) of the pure ILs and of non-neutralized and neutralized IL-loaded (75%) and nonloaded films were performed using TGA-Q500 (TA Instruments) equipment. Measurements were conducted by heating the samples from room temperature up to 600 °C at a heating rate of 10 °C min^{-1} and under flowing nitrogen. Differential scanning calorimetry (DSC) analyses of the pure ILs were performed using DSC-Q100 (TA Instruments) equipment. Samples (approximately 7−10 mg weight) were sealed in aluminum pans with a pinhole. An inert atmosphere was maintained by purging nitrogen at the flow rate of 50 mL min^{-1}, and all measurements were carried out by consecutive heating, cooling, and reheating runs. Modulated differential scanning calorimetry (MDSC) curves were obtained from the reheating run at 2 °C min^{-1} from −80 to 250 °C with a modulation amplitude period of 60 s and a modulation amplitude of 0.318 °C. In both cases, samples were maintained in a desiccator at room temperature and 20% RH before analysis to achieve better reproducibility. Mechanical tests were carried out in tensile mode using a texture profile analyzer (TA-XT Express, Stable Micro Systems Ltd., U.K.) at room temperature for non-neutralized IL-loaded (75%) and nonloaded CS films (which were conditioned at ≈90% HR before analysis and cut in "dog-bone" shape). The initial gauge length and testing speed were 15 mm and 0.1 mm/s, respectively (for a test distance of 10 mm and 0.1 g trigger force). The thickness of each film was measured at three different points using a digital micrometer (Mitutoya, model MDC-25S, Japan). The elastic modulus was calculated from the initial slope (between 0.05% and 0.25%) of the stress−strain curves.

Impedance Measurements. Electrochemical impedance spectroscopy (EIS) experiments were carried out using a PGSTAT 30 potentiostat−galvanostat with a frequency response analyzer (FRA2) module controlled by FRA software version 4.9 (EcoChemie, Utrecht, The Netherlands). A r.m.s. perturbation of 350 mV was applied over the frequency range between 1.0 MHz and 0.1 Hz (with 10 frequency values per decade). Spectra were recorded at 0.1 V and fitted using electrical equivalent circuits (with ZView 3.2 software, Scribner Associates Inc., U.S.A.). For this purpose, and 48 h before measurements, samples were placed at the maximum RH achieved at room temperature (≈ 85%). "Dry" films were then sandwiched between two blocking electrodes (1 cm^2, S136 steel) in the measurement cell in air. A fixed electric tension of 0.1 V, on top of which the AC voltage was superimposed, was applied between the two electrodes. Measurements were performed for IL-loaded (75%) and nonloaded neutralized and non-neutralized CS films. The influence of the amount of IL loaded on the impedance of the films was studied for the non-neutralized and (25, 50, and 75%) [Ch][Cl]-loaded films.

Preliminary Actuation Tests with AC current. IL-loaded (75%) and nonloaded CS films (10 × 40 × ∼0.1 mm) were covered with gold on both sides using the same sputter-coating conditions previously described for SEM analysis. It was considered that the thickness of the gold electrodes was extremely thin and did not affect the bending stiffness of the tested films. The actuator was firmly supported vertically in air (at 80−90% RH and room temperature) and was left to equilibrate. An initial bending was detected and attributed to the structural reorganization of the polymer chains that result from the absorption of water vapor molecules. When no further displacement was detected, an AC source/pulse generator (Wavetek 166, USA) was used to produce a sinusoidal signal ranging from to −15 to +15 V and 10 Hz frequency. Bending displacements were measured using a high precision laser Doppler vibrometer (Baumer OADM 20I4460/S14C,

Germany). During measurements, the RH and temperature conditions in the experimental setup were continuously monitored using a hygrometer.

Release Kinetics of DXA at Different pH Conditions. Sodium phosphate dexamethasone (DXA) release kinetic studies were performed spectrophotometrically (UV−vis spectrophotometer, V550, Japan) by monitoring the maximum absorbance of the drug at 242 ± 2 nm. Three buffers (of different pH: 4, 7, and 10) were used as the release media (at fixed ionic strength, 0.1 M). Square film samples (1 cm^2, previously stored at 20% RH) were introduced into a dialysis membrane (Spectra/Por Dialysis membrane, MWCO 8000) that was sealed with Teflon on both sides. Each sample was immersed in 20 mL of release media, and release experiments were carried out at 37 °C under orbital stirring (100 rpm). The sample weight/release solvent volume ratio was previously optimized in order to avoid DXA saturation of the release solution. At predefined time intervals, aliquots with 3 mL were taken from the release solutions, analyzed, and returned into the release media. Measurements were carried out until a constant release profile was achieved. Released DXA concentrations were calculated using previously determined calibration curves with coefficients of determination (r^2) higher than 0.999 in all cases (using solutions of DXA with known concentration in the three buffer solutions, at 37 °C). All the release assays were carried out in duplicate. Measurements were performed for [Ch][DHP]-loaded (75%) and nonloaded neutralized CS films.

RESULTS AND DISCUSSION

The water vapor sorption (WVS) and water vapor permeability (WVP) capacities of nonloaded and IL-loaded CS films were studied in this work because hydration is known to significantly affect charge diffusion through polymeric hydrogel films[42] and their actuation capacities, as well as their mechanical and thermal properties.[43,44] Neutralized and non-neutralized films were also studied to account for the neutralization procedure influence on the measured properties. Figure 1 compares the WVS profiles of IL-loaded and nonloaded films before and after neutralization for a monitoring period of 8 h (Figure 1a) and at equilibrium after 48 h (Figure 1b).

Results show that non-neutralized films achieve WVS equilibrium much faster than neutralized ones (for which equilibrium is attained only after 48 h). This effect is most probably due to electrostatic repulsion between CS amino groups that become protonated ($-NH_3^+$) as the amount of water inside the matrix increases. These repulsions lead to an increase in free volume between polymer chains that permit the accommodation of higher amounts of water inside the polymeric structure. In addition, the osmotic charge gradient between the liquid water inside CS films and the water vapor phase is so high that it will also contribute to the sorption of more water vapor. On the contrary, neutralized films present more sustained WVS profiles because of the higher degree of physical reticulation (mainly hydrogen bonding) that may occur between amino ($-NH_2$) and hydroxyl (−OH) groups that make permeation of water vapor molecules into the CS matrix difficult.[11] In this case, the osmotic charge gradient is lower than in the case of non-neutralized films that also leads to lower and slower water vapor sorption. The addition of ILs (to non-neutralized and neutralized CS films) did not significantly affect the equilibrium WVS capacity of the prepared films. This is probably due to the hydrophilic and hygroscopic nature of CS by itself. While CS films loaded with [Ch][DHP] present increased equilibrium (48 h) WVS capacities (around 13% higher for both neutralized and non-neutralized films), this did not happen for films loaded with [Ch][Cl]. In this case, IL addition did not seem to affect the WVS equilibrium for non-neutralized films, but it led to a WVS decrease for neutralized films.

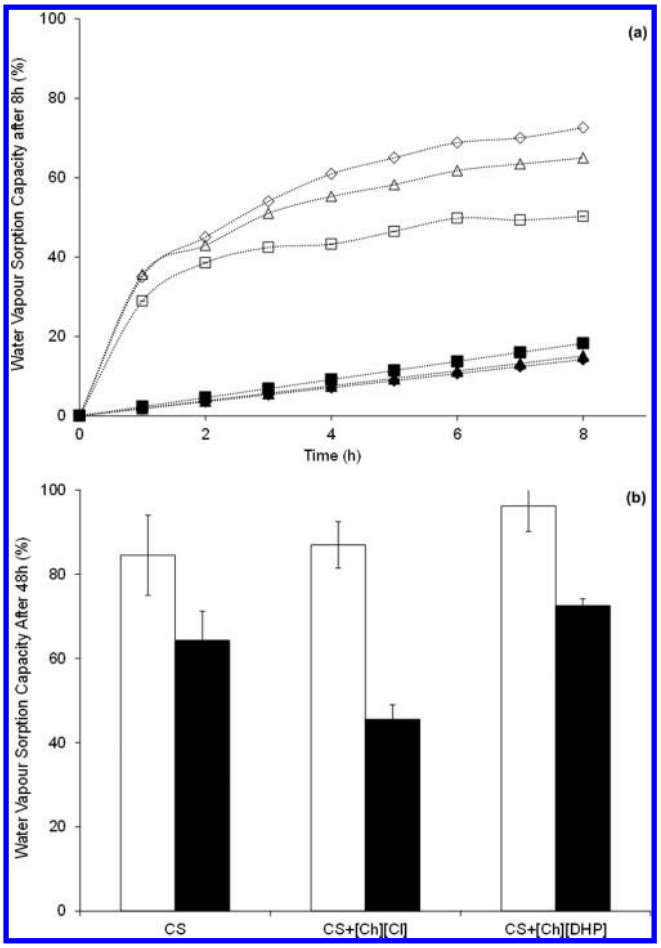

Figure 1. Water vapor sorption capacity for nonloaded CS films (squares) and for films loaded with [Ch][Cl] (diamonds) and [Ch][DHP] (triangles) during the first 8 h monitoring period (a) and at equilibrium after 48 h (b). Neutralized films are represented by full symbols/black bars and non-neutralized films by open symbols/white bars. Experiments were carried out at 37 °C and in a 90% relative humidity (RH) environment.

The influence of the IL addition was even more evident in the values of water vapor transmission rate and permeability (Table 1). The WVTR value obtained for neutralized nonloaded CS films is similar to previous data reported in the literature (50 g h^{-1} m^{-2}) obtained under similar experimental conditions (84% RH and 25 °C). The WVP of non-neutralized CS films loaded with ILs increases similarly for both ILs, while that for neutralized films decreases for films loaded with [Ch][Cl] and significantly increases (more than twice) for films loaded with [Ch][DHP]. Further studies are needed in order to understand if the observed decrease for [Ch][Cl]-loaded neutralized CS films is due to IL leaching during the neutralization step or if there are any other phenomena involved in the process. Nevertheless, these tendencies are in agreement with those described above for the WVS capacities of the films because swelling (which is induced by water vapor sorption) may lead to conformational changes in the film microstructure, thus creating pathways in the polymeric structure that will enhance permeation. This effect is particularly important for cationic hydrophilic polymers (such as CS) for which water vapor molecules can interact

Table 1. Water Barrier Behavior (water vapor transmission rate (WVTR) and water vapor permeability (WVP)) and Thermal Stability (peak temperature (*Tp*) from DTG curves) of Non-Neutralized and Neutralized Chitosan Films Alone (CS) and for Films Loaded with 75% [Ch][Cl] and 75% [Ch][DHP]

IL		thickness (mm)	WVTR (g h^{-1} m^{-2})	WVP (10^{-6}) (g $h^{-1}m^{-1}kPa^{-1}$)	weight loss at 100 °C (%)	T_p[a] (°C)
–	non-neutralized	0.114	43.14 ± 1.87	8.67 ± 0.38	13.57 ± 0.77	287.2 ± 7.3
[Ch][Cl]		0.118	62.00 ± 1.78	12.92 ± 0.04	14.28 ± 0.51	264.6 ± 3.9
[Ch][DHP]		0.108	59.03 ± 1.97	11.28 ± 0.58	7.91 ± 0.39	251.5 ± 1.1
–	neutralized	0.078	53.04 ± 3.34	7.32 ± 0.46	3.22 ± 0.49	294.6 ± 0.9
[Ch][Cl]		0.069	48.82 ± 1.86	5.96 ± 0.23	3.41 ± 0.20	296.7 ± 0.7
[Ch][DHP]		0.128	67.99 ± 3.40	15.40 ± 0.77	2.10 ± 0.40	291.3 ± 0.8

[a]Defined as the maximum temperature obtained from the first derivative of weight loss as a function of temperature (DTG).

favorably with the polymeric matrix, plasticize, and increase the flexibility of the polymeric chains.[43,44] A similar behavior was already reported after the incorporation of hydrophilic plasticizers into protein and polysaccharide films that resulted in an increase in their WVP.[45,46] In the present work, the ILs employed also seem to work as plasticizer additives that facilitate the diffusion of water molecules through the film structure. This occurs not only by changing the WVS capacities of the films but also because the inclusion of IL molecules into the polymer network increases the interchain distance (by reducing intermolecular interactions), thus facilitating the diffusion of water molecules through the film. This plasticizing effect of ILs was further confirmed by mechanical analysis. A significant decrease in the elastic modulus was observed from 13 MPa for nonloaded CS to <1 and 2 MPa for [Ch][Cl]- and [Ch][DHP] CS-loaded films, respectively, which confirms the higher flexibility of IL loaded CS films. IL-loaded films were also visually more rubbery than nonloaded ones.

The macroscopic and molecular structural changes induced by the presence of ILs were confirmed by SEM (Figure 2) and by thermogravimetric analysis (Table 1).

In the first case, the cross section micrographs of non-neutralized films show that the structure of nonloaded CS seems to be denser than IL-loaded films. On the other hand, [Ch][DHP]-loaded films seem to be denser than [Ch][Cl]-loaded films (Figure 2c).

The presence of ILs also induces a decrease in the maximum degradation temperature of non-neutralized CS films (T_p in Table 1), which indicates that ILs affect the intrinsic reticulation of the polymer structure (due to the number of hydrogen bonding and to electrostatic interactions) and may disrupt its structure.[47−49] This effect seems to be more pronounced for [Ch][DHP]-loaded films and for non-neutralized films (Table 1), which is in good agreement with the previously discussed data.

The effect of choline-based ionic liquids on the electro-responsiveness of CS films was measured by AC impedance spectroscopy using a symmetrical cell with two steel electrodes. CS films were previously stored at 80% RH for 48 h before measurements because ion diffusion is enhanced at higher hydration levels.[42] Moreover, measurements were performed for both neutralized and non-neutralized CS films in order to account for the influence of residual acetic acid on the impedance of the films.

Impedance spectra of non-neutralized CS films loaded with different amounts of [Ch][Cl] are shown in Figure 3. As can be observed, nonloaded CS films present the more resistive behavior, which decreases as the amount of loaded [Ch][Cl] increases. The spectra measured for CS and for CS loaded with 25% of [Ch][Cl] present a small semicircle in the high

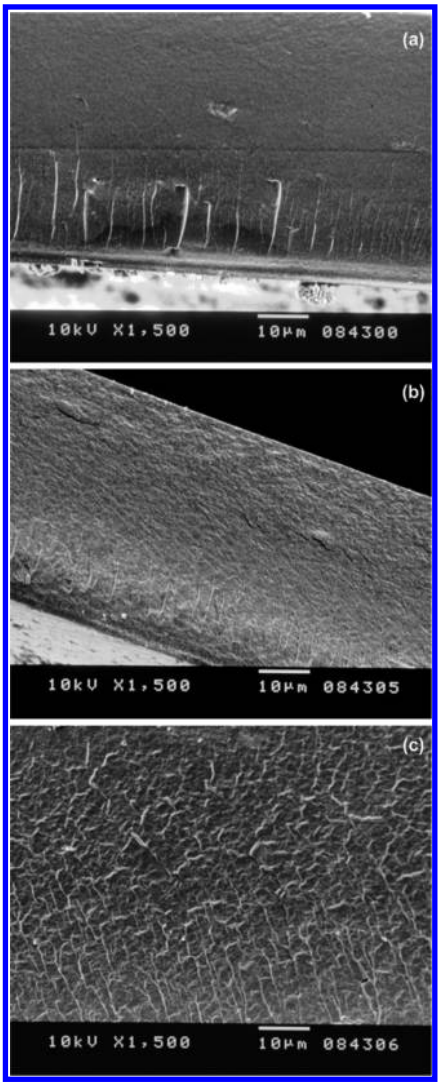

Figure 2. Cross section SEM micrographs for non-neutralized CS films: nonloaded (a), loaded with 75% [Ch][Cl] (b), and loaded with 75% [Ch][DHP] (c).

frequency region (inset of Figure 3), which is related to the charge transfer reaction and to double layer capacitance. Films loaded with 50% and 75% [Ch][Cl] begin directly with diffusive ≈45° lines at high frequency, all of them ending with capacitive lines and showing an increase in the angle corresponding to capacitance with greater IL content. All the equivalent circuits used to fit the spectra contained a cell resistance, *RΩ*, which comprises the resistances of the two steel electrodes of the electrical contacts and wires and that of the

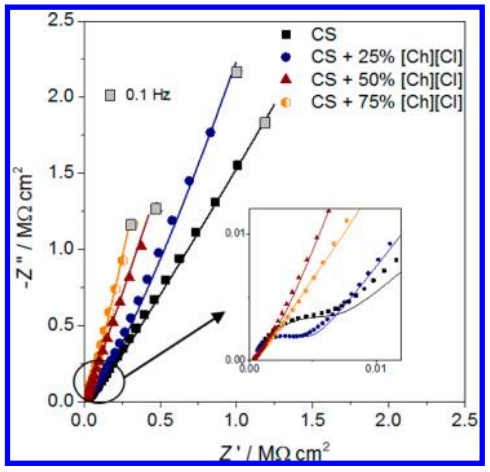

Figure 3. EIS spectra recorded for non-neutralized CS films: nonloaded and CS+25%, 50%, and 75% [Ch][Cl]-loaded films. Applied potential +0.1 V and varying frequencies from 0.1 to 10^6 Hz. Lines show equivalent circuit fitting.

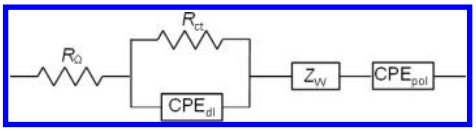

Figure 4. Equivalent circuit used to fit the spectra in Figure 3, 5, and 7.

film placed between the electrodes. Because beside the film all the other resistance contributions can be considered constant, the differences in $R\Omega$ may be attributed to the ohmic resistance of the film. In the case of non-neutralized CS films, $R\Omega$ decreases with the [Ch][Cl]-loaded amount and varies from 0.79 kΩ cm^2 (for nonloaded CS) to 0.28 kΩ cm^2 (for CS+75% [Ch][Cl]), as shown in Table 2.

When comparing between ILs, the $R\Omega$ value obtained for films loaded with [Ch][DHP] (at the same loaded amount, 75%) is higher (0.67 kΩ cm^2) than that of [Ch][Cl] although still lower than that of unloaded CS. Neutralization of nonloaded and IL-loaded CS films leads to a significant increase in the $R\Omega$ values to 1.59 kΩ cm^2 for CS and 1.34 kΩ cm^2 and 2.97 kΩ cm^2 for CS+75% [Ch][Cl] and CS+75% [Ch][DHP], respectively. The equivalent circuit used to fit the spectra for nonloaded CS and CS+25% [Ch][Cl] (Figure 4), comprised a parallel combination of a charge transfer resistance, R_{ct}, with a double layer non-ideal capacitance, expressed as a constant phase element, CPE_{dl} (to fit the semicircle in the high frequency region of the spectra). This parallel combination is in series with a Warburg resistance, Z_w (for intermediate frequency) and a polarization capacitance, CPE_{pol} (for the low frequency region). The equivalent circuit used to fit the spectra of CS+50% and CS+75% [Ch][Cl] contained only the Z_w and CPE_{pol} components.

The Warburg diffusional element, Z_W, is described by eq 3

$$Z_W = R_D\left[\frac{\mathrm{ctg}(j\varpi\tau_D)^{1/2}}{j\varpi\tau_D^{1/2}}\right] \quad (3)$$

and is characterized by a diffusional time constant (τ_D), a diffusional pseudocapacitance (C_D) and a diffusion resistance ($R_D = \tau_D/C_D$).[50]

The constant phase element is expressed by CPE = $\{(Ci\omega)^\alpha\}^{-1}$, where C is a constant, i is the square root of −1, ω is the angular frequency, and α is an exponent that can vary between 1.0 (for uniform surfaces) and 0.5 (for porous electrodes); it thus reflects the material's nonuniformity and surface roughness.[51] Table 2 summarizes the resistive and capacitive elements estimated by fitting the impedance spectra to the equivalent circuit model shown in Figure 4.

As can be seen, R_{ct} and Z_w values for CS+25% [Ch][Cl] films are lower than those of nonloaded CS films. On the contrary, CPE_{DL} and CPE_{pol} fitted values are higher. This means that a decrease in the charge transfer resistance at the electrode−biopolymer interface occurs when [Ch][Cl] is added to CS. Moreover, an increase in both the double layer and polarization capacitance values also occurs. For CS films loaded with 50 and 75% [Ch][Cl], the later present the lowest Z_w values (33 kΩ cm^2 s$^{\alpha-1}$), which may indicate that there is a specific range for the number of available charges (charges from both CS and [Ch][Cl]) that favors their diffusion within the polymer. It was also observed that the CPE_{pol} values increase systematically with the amount of [Ch][Cl] (from 110.1 to 280.0 nF cm^{-2} s$^{\alpha-1}$), although values for CS+50% and 75% of [Ch][Cl] are very similar. In addition, α_3 values are also increasing (from

Table 2. Equivalent Circuit Element Values Obtained from Fitting the Spectra Shown in Figures 3 and 7 for Non-Neutralized and Neutralized as Well as for Nonloaded and IL-loaded CS films[b]

	system	R_Ω kΩ cm^2	R_{ct} kΩ cm^2	CPE_{dl} nF cm^{-2} s$^{\alpha-1}$	α_1	Z_W kΩ cm2 s$^{\alpha-1}$	τ_D s	α_2	CPE_{pol} nF cm^{-2} s$^{\alpha-1}$	α_3
non-neutralized	CS	0.79 (0.02)	29.8 (8.92)	0.11 (3.84)	0.93 (0.70)	124.6 (4.02)	0.010 (0.01)	0.43 (0.20)	110.1 (2.36)	0.60 (0.11)
	CS+25% [Ch][Cl]	0.63 (0.08)	20.9 (6.50)	0.20 (2.72)	0.90 (0.83)	3.7 (9.13)	0.001 (0.02)	0.49 (0.66)	150.2 (3.11)	0.62 (0.15)
	CS+50% [Ch][Cl]	0.44 (0.06)	–	–	–	131.3 (4.27)	0.030 (0.01)	0.46 (0.32)	279.5 (1.71)	0.72 (0.12)
	CS+75% [Ch][Cl]	0.28 (0.07)	–	–	–	33.1 (4.41)	0.004 (0.01)	0.43 (0.23)	280.0 (3.82)	0.75 (0.14)
	CS+75% [Ch][DHP]	0.67 (0.01)	0.015 (7.01)	2400.0 (2.80)	0.59 (0.12)	–	–	–	403.9 (2.89)	0.83 (0.23)
neutralized	CS	1.59 (0.04)	286.3 (5.78)	0.01 (1.23)	0.96 (0.45)	2390.1 (7.48)	0.098 (0.03)	0.43 (0.23)	27.3 (6.12)	0.68 (0.12)
	CS+75% [Ch][Cl]	1.34 (0.01)	–	–	–	108.5 (7.17)	0.023 (0.01)	0.49 (0.04)	190.2 (3.01)	0.68 (0.33)
	CS+75% [Ch][DHP]	2.97 (0.04)	1.4 (8.90)	0.02 (0.04)	0.87 (0.53)	–	–	–	52.5 (1.03)	0.69 (0.17)

[b]Values between parentheses correspond to the fitting error (%). Fitting error = (calculated − experimental)/experimental ×100.

0.60 to 0.75) with an increase in the [Ch][Cl] amount, which suggests that the loaded biopolymer becomes more conductive and homogeneous (in terms of charge distribution) with an increase in the amount of loaded [Ch][Cl]. Finally, there are no significant differences in α_1 and α_2 values, which indicate surface and bulk homogeneity of the films.

The influence of the type of IL on the impedance of non-neutralized CS-loaded films is shown in Figure 5. The

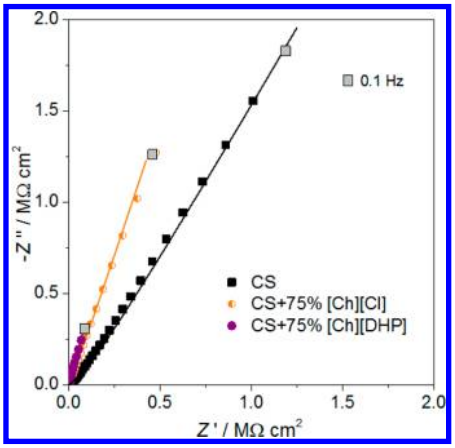

Figure 5. EIS spectra recorded for non-neutralized and nonloaded CS, CS+75% [Ch][Cl], and CS+75% [Ch][DHP] films. Applied potential +0.1 V and varying frequencies from 0.1 to 10^6 Hz. Lines show equivalent circuit fitting.

corresponding fitting results are presented in Table 2. CS films loaded with 75% [Ch][DHP] show a very small semicircle in the high frequency region, a very low R_{ct} (15.0 Ω cm^2), and a very high CPE_{pol} value (403.9 nF cm^{-2} s$^{\alpha-1}$). This value is much higher than that obtained for films loaded with 75% [Ch][Cl] (CPE_{pol} = 280.0 nF cm^{-2} s$^{\alpha-1}$), which clearly indicates that conductivity is enhanced when using [Ch][DHP]. This may happen due to the specific properties of [Ch][DHP]. The ionic conductivity of many plastic crystals (such as [Ch][DHP]) usually presents a relatively large increase at temperatures near their solid−solid phase transition temperatures, which is considered to be due to an increased number of charge carriers having higher mobilities (arising from the increased rotational and/or translational motions). This behavior was already observed for pure imidazolium and pyrrolidinium-based ILs.[39,40]

However, this behavior was not noticed for pure [Ch][DHP].[40] Therefore, additional studies should be carried out in order to conclude if the ion mobilities (induced at the low temperature solid−solid transition (23.5 °C)) potentiate charge transfer when the IL is confined by CS chains. In fact, when comparing the DSC thermal profiles of the pure ILs (Figure 6), it can be observed that both ILs present two solid−solid phase transitions, which correspond to disorder or to plastic crystal phase transitions (at 23.5 and 122.4 °C for [Ch][DHP] and at −9.1 and 67.2 °C, for [Ch][Cl]). Results obtained for [Ch][DHP] confirm that this IL presents a plastic crystalline phase with slightly higher thermal stability (~100 °C) than [Ch][Cl] (~ 67 °C). Moreover, [Ch][DHP] presents a solid−solid phase transition around room temperature (23.5 °C) that may affect the structural reorganization of the IL−CS system and justify the impedance results obtained (enhanced conduction) measured at similar temperature for CS films doped with this IL.

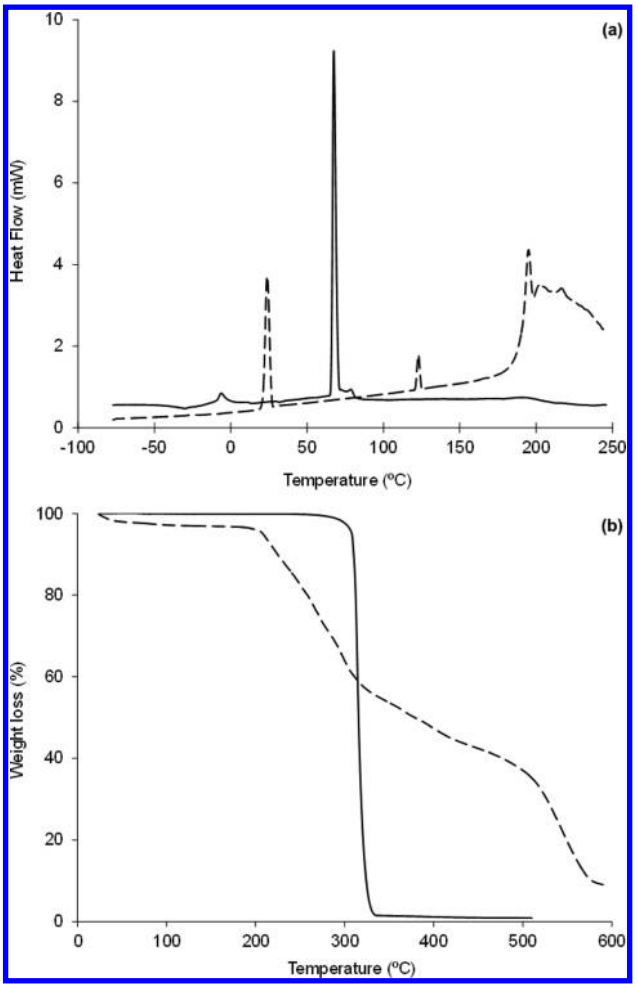

Figure 6. DSC (a) and TGA (b) profiles for pure [Ch][Cl] (full lines) and pure [Ch][DHP] (dashed lines).

The melting/degradation temperatures of the pure ILs were determined by thermogravimetric analysi,s and they were equal to 194.3 and 315.7 °C for [Ch][DHP] and [Ch][Cl], respectively (Figure 6).

This analysis also showed that [Ch][DHP] is slightly more hydrophilic than [Ch][Cl] (higher weight losses at 110 °C), which in turn presents higher thermal stability (~315 °C) than [Ch][DHP]. Similar results (DSC and TGA) were previously reported in the literature for [Ch][DHP];[49] however, and to our knowledge, there is no previous data measured for [Ch][Cl].

The effect of residual acetic acid on the impedance of nonloaded and IL-loaded (75%) films was also studied, and the results are compared in Figure 7 a and b.

The corresponding equivalent circuit element values are given in Table 2. Results show that neutralized nonloaded CS films and CS+75% [Ch][DHP] are significantly more resistive than the non-neutralized ones. For nonloaded CS, neutralization leads to an increase of R_{ct} from 29.8 to 286.3 kΩ cm^2 and to a decrease of both CPE_{dl} and CPE_{pol} (from 0.11 to 0.01 and 110.1 to 27.3 nF cm^{-2} s$^{\alpha-1}$, respectively). For CS+75% [Ch][DHP], the neutralization procedure led to even more drastic changes: R_{ct} increased from 0.015 to 1.4 kΩ cm^2, CPE_{dl} decreased from 2400.0 to 0.021, and CPE_{pol} decreased from 403.9 to 52.5 nF cm^{-2} s$^{\alpha-1}$. These results clearly indicate that the presence of residual acetic acid is enhancing the

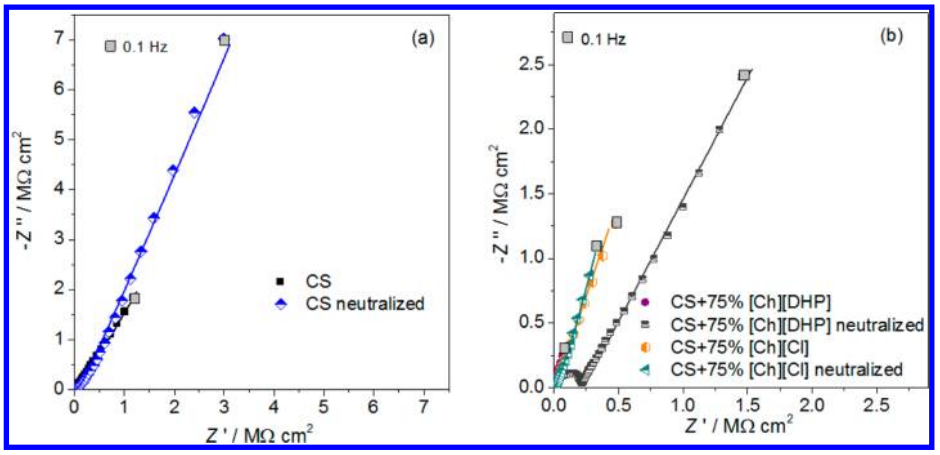

Figure 7. EIS spectra recorded for nonloaded, neutralized, and non-neutralized CS films (a) and for neutralized and non-neutralized CS+75% [Ch][Cl]/[Ch][DHP] loaded films (b). Applied potential +0.1 V and varying frequencies from 0.1 to 10^6 Hz. Lines show equivalent circuit fitting.

conductivity of the films (with and without the addition of ILs). This may be mostly because under these conditions CS amino groups are protonated ($-NH_3^+$), and therefore, the density of positive charges along the matrix is increased, which consequently enhances the diffusion of charges through the polymeric matrix. Small changes in film response were observed for the CS+75%[Ch][Cl] system, both non-neutralized and neutralized, the tendency being the same as for the films discussed previously: Z_w increased from 33.1 to 108.5 kΩ cm^2 $s^{\alpha-1}$ and CPE_{pol} decreased from 280.0 to 190.2 nF cm^{-2} $s^{\alpha-1}$.

Previous studies reported in the literature showed that the amount of water as well as medium acidity has a strong influence on CS conductivity because the water molecules located around the hydronium ions (H_3O^+) can support ion diffusion throughout the system.[52−54] The proposed mechanism for ionic conductivity considers that when water is incorporated into a CS film some amino groups become protonated leading to the formation of hydroxide ions. Because the NH_3^+ groups are bonded to the CS backbone, only OH^- ions are then free to move under the action of an AC signal. In acidic solutions, besides simple diffusion and migration of hydronium ions (vehicle mechanism), proton transport can also occur by proton hopping between hydrogen-bonded water molecules and hydronium ions (Grotthuss mechanism). In this case, the transport of the proton in the film can occur from a protonated molecule to a nonprotonated molecule or from the neighboring proton to the proton defect site.[53,55] The idea of using proton carriers, other than water molecules, to achieve fast proton conduction through CS films has been attempted by doping CS films with imidazolium based ILs[29,30] or phosphoric acid.[56] This helps to improve proton conduction in CS highly viscous systems for which proton transport through the vehicle mechanism may be decelerated (by means of the Grotthuss-type mechanism).

In the present work, it was intended to evaluate the capacity of [Ch][DHP] to work as an efficient, biodegradable, and biocompatible alternative additive to induce Grotthuss-type proton conduction mechanism throughout CS films. Comparison was done with [Ch][Cl] for which conduction is expected to occur mainly by a diffusion vehicle mechanism,[29] considering differences in anion sizes and possible interactions with the CS matrix (hydrogen bonding is only possible in the case of [Ch][DHP] for instance). It has been previously reported that the $[DHP]^-$ anion may provide a mechanism for fast proton hopping, either through a Grotthuss mechanism via structural diffusion[40,57] or through a paddle wheel mechanism that involves both the cation and the anion.[58] It was also demonstrated that the conductivity increases significantly (by almost 3 orders of magnitude at room temperature) upon the addition of phosphoric acid,[41,59] which indicates that the ionic conductivity in acidic/[choline][DHP] mixtures is due to contributions from all the ionic species (H^+, $[choline]^+$, and $[DHP]^-$). These findings are in good agreement with the impedance results that were obtained in this work and that showed that the conductivity of [Ch][DHP]-loaded CS films was more affected (significantly decreased) by the acidic conditions of the media than [Ch][Cl]-loaded CS films.

Taking into account the enhanced response of CS films loaded with both ILs at non-neutralized conditions, it was attempted to preliminarily study their actuation capacities when stimulated by a low electrical AC current. Non-neutralized IL-loaded (75%) and nonloaded CS films were covered with gold to increase the specific area of the electrodes and the electrochemical capacitance and also to provide ionic transportation channels during the electrochemical charging and discharging processes.[60] The films flexion distance variation with time is presented in Figure 8. Results showed that both ILs increased the maximum flexion distance that can be achieved when induced by the same applied electrical current. Under the same experimental conditions (~90% RH and room temperature), the maximum displacement measured for nonloaded CS films was equal to 1.03 mm, while that for CS films loaded with [Ch][Cl] and [Ch][DHP] was 1.54 and 2.49 mm, respectively.

It has been previously reported that in acidic and hydrated conditions protonated amino groups ($-NH_3^+$) cannot move freely, but acetic acid anions (CH_3COO^-) are free to move, leading to bending.[61] The higher displacement observed in this work for IL-loaded films and mainly for [Ch][DHP] may thus result from the enhanced ion transport mechanism promoted by this IL and as previously discussed. The non-ideal sinusoidal displacement vs time curve obtained in all cases at the tested frequency and voltage conditions may be justified by the difficulty that the ions find to return to the initial stationary position, probably due to strong electrostatic interactions that may be established within the film but also to its dense structure.

The release of a drug from a polymeric matrix is often a diffusion-dependent process that is largely influenced by the

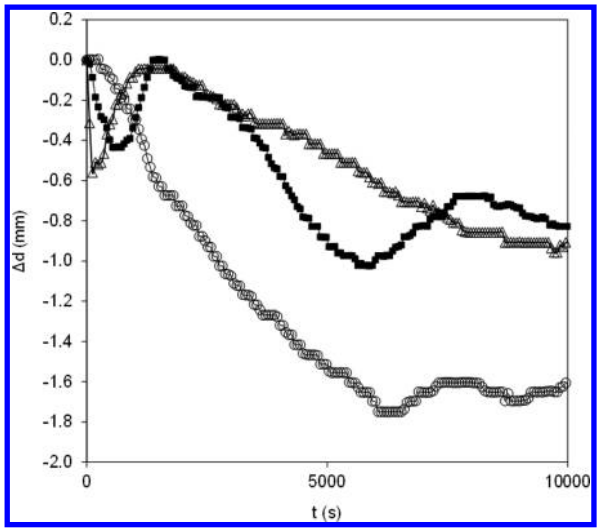

Figure 8. Bending displacement (mm) measured for non-neutralized CS films as a function of time: nonloaded CS films (■), CS films loaded with 75% [Ch][Cl] (Δ), and with 75% [Ch][DHP] (○).

swelling capacity of the matrix and where higher swelling capacities usually lead to higher and/or faster release rates. The equilibrium water swelling capacities of IL-loaded and non-loaded CS films, obtained at different pH conditions and ionic strengths and after 8 h of swelling, are presented in Figure 9.

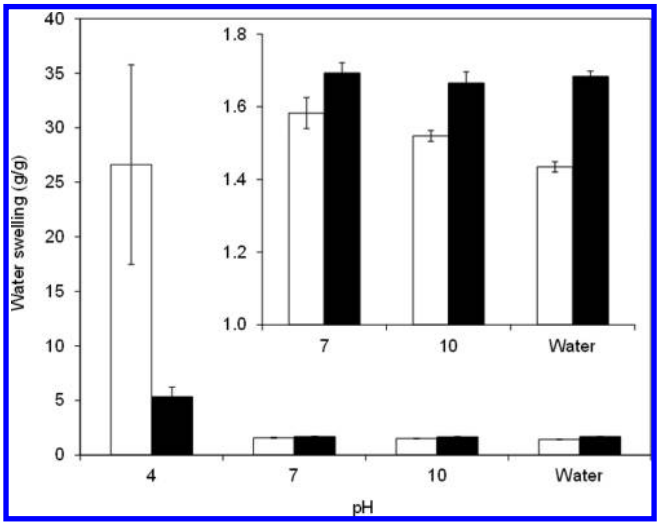

Figure 9. Equilibrium water swelling capacities (WSC) obtained after 8 h for neutralized and nonloaded (white) and neutralized and 75% [Ch][DHP]-loaded CS films (black), measured at 37 °C in different pH and constant ionic strength (0.1 M) conditions.

Taking into account the envisaged applications and the results already obtained, this study was performed just for nonloaded and 75%[Ch][DHP]-loaded CS films, neutralized in both cases, which are the conditions that originated the most stable films. As expected (and because the ionic strength of the swelling media was kept constant), nonloaded CS films present a significantly higher swelling capacity (WSC) at pH 4 (26.6 ± 9.1 g/g) compared to values obtained at pH 7 (1.58 ± 0.04 g/g) and at pH 10 (1.52 ± 0.01 g/g). This is mostly due to the increased charge density inside the polymeric matrix, which causes electrostatic repulsions between CS chains (which are protonated, $-NH_3^+$), and to the increased osmotic charge gradient between the polymeric environment and the media environment, which favors the swelling process, as more water molecules will enter the polymer in order to "dilute" this high charge density. At higher pH values, most of the CS amino groups are in the neutral form ($-NH_2$), and therefore, the ionic repulsions and the osmotic charge gradient are minimized at pH 7 and are almost inexistent at pH 10. In addition, under these conditions, hydrogen bonding between the CS hydroxyl and amine groups can be established, leading to physical reticulation between polymer chains, which may also help to explain the significantly lower WSC values that were obtained. Even if some IL is leached during the neutralization step, the effect of [Ch][DHP] on the swelling capacity of the films is clear. In fact, the presence of [Ch][DHP] influences the WSC of the films in distinct ways, depending on the pH of the swelling medium. A clear decrease in the water swelling capacity occurs at lower pH values (~ 80%) while a small increase is observed at pH 7 (~7%) and at pH 10 (~10%). At pH 7, an increase in the WSC would be expected because the number of charges inside the matrix increases (compared to the nonloaded films) and swelling would compensate the change in the osmotic charge gradient. However, in the present case, it seems that the IL anion may be "shielding" the protonated amino groups and consequently decreasing the electrostatic repulsions that would favor swelling.[62] Moreover, there may also exist some additional physical reticulation between the CS polymer chains similarly to the case that was recently reported by Vijayaraghavan and coauthors, who demonstrated the feasibility of using choline salts (including [Ch][DHP]) as biocompatible cross-linking agents for collagen-based materials.[35] On the other hand, IL-loaded films present a slight and similar increase in their water swelling capacities (~7% at pH 7 and ~10% at pH 10). At these pH values, the number of amino groups ($-NH_2$) is higher than the number of $-NH_3^+$ groups, and the presence of the IL ions inside the matrix may induce the separation of the polymer chains (creation of free volumes), which facilitates the permeation of water into films and the exchange of charges between the polymeric matrix and the buffer solution (to achieve Donnan equilibrium). The influence of the salts in the buffer solutions was also confirmed by measuring the WSC in Milli-Q water (Figure 9). The pH of distilled water usually varies between 5.5 and 6.5 due to dissolution of carbon dioxide and the consequent formation of carbonic acid. At this pH, only part of the CS amino groups are in the protonated form ($-NH_3^+$). However, the number of these protonated groups is much lower than at pH 4. Therefore, in water, the osmotic charge gradient between the polymer and the swelling media will not be very high, and the nonloaded polymer will not swell as much as at pH 4.0. On the other hand, and for loaded films, the addition of [Ch][DHP] will increase the charge density inside the polymer and the osmotic charge gradient. In result, IL-loaded films present higher WSC values (15%) than nonloaded films.

One of the aims of this study was to evaluate the effectiveness of ILs as agents that can change the electrostatic interactions between the ionic drugs and the CS polymeric network and consequently influence the release profiles of these drugs. The release profiles obtained for neutralized [Ch][DHP]-loaded (75%) and nonloaded CS films at different pHs (and at fixed ionic strength, 0.1 M) are shown in Figure 10. Considering the pK_a of DXA (pK_{a1} and pK_{a2} at pH 2.04 and 6.0, respectively)[63] and of chitosan (pK_a is 6.3–6.5),[64,65]

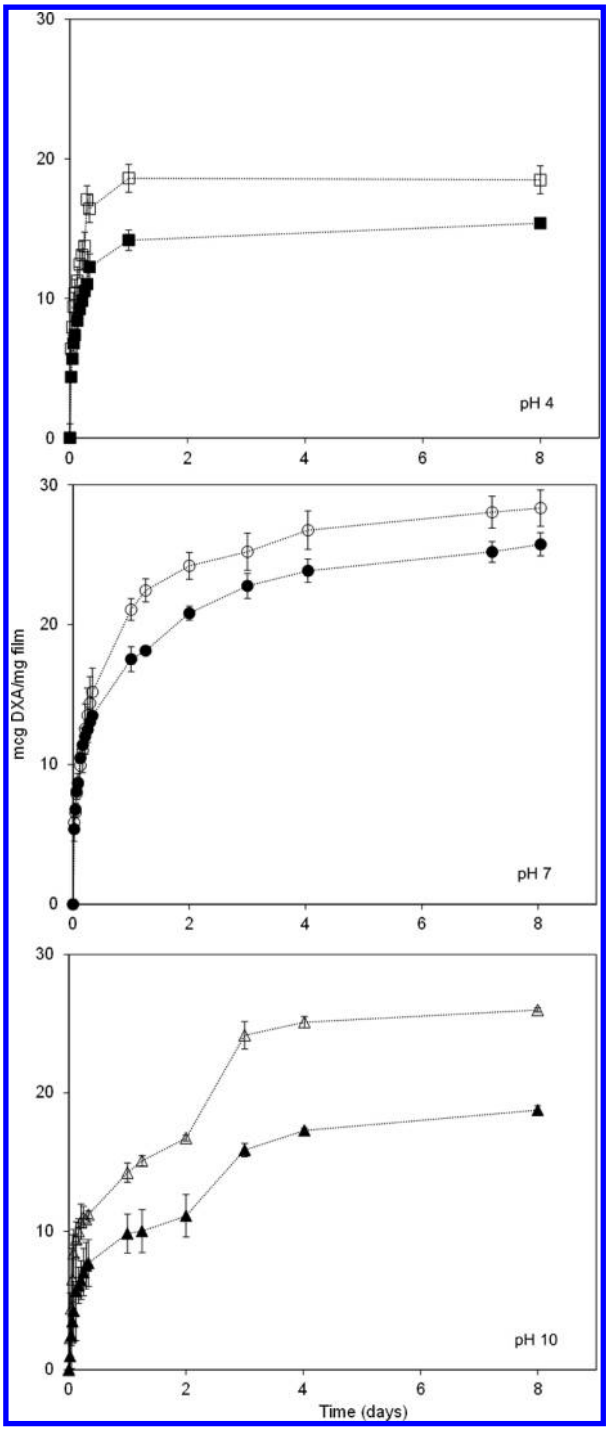

Figure 10. DXA cumulative released amounts during 8 days from neutralized CS films: nonloaded films (open symbols) and 75% [Ch][DHP]-loaded films (full symbols). Experiments were performed at 37 °C and at pH 4 (top), pH 7 (middle), and pH 10 (bottom). Lines serve only as guides for the eye.

different ionic species may be present depending on the release media employed, as shown in Figure 11.

Therefore, at pH 4, DXA may interact favorably with CS through ionic and hydrogen bonding (because DXA is partially ionized with negatively charged $-COO^-$ groups and CS is strongly ionized with positively charged $-NH_3^+$ groups). However, at pH 7 and pH 10, only hydrogen bonding prevails because the amino groups in CS are in the neutral form ($-NH_2$). These facts may justify the lower total released amounts of DXA observed at pH 4 (~ 62% of the total loaded DXA because DXA is strongly linked to CS) compared to the DXA release values at pH 7 (~ 95%) and at pH 10 (~ 90%) (considering that the total loaded amount of DXA is equal to 30 μg/mg polymer). Moreover, at the higher values of pH, DXA will also contribute additional charges to the polymeric matrix, which will further enhance water swelling (to compensate the osmotic charge gradient) and consequently the release of DXA.

The amount of DXA released from films loaded with [Ch][DHP] is always lower than for films without IL, independent of the pH of the release medium. These differences are around 17% at pH 4, 10% at pH 7, and 28% at pH 10. Thus, the addition of [Ch][DHP] seems to help to retain the drug in the CS matrix, and therefore, it may work as an additional variable that can be used to tune the sustained delivery of ionic drugs. Although the mechanism is not yet completely understood (due to the large number of variables that can affect the process), it can be assumed that [Ch][DHP] may be interacting simultaneously with DXA and the CS matrix. Further studies will be performed in order to reach conclusions about these potential drug–IL–chitosan interactions. These results also make it clear that the release of DXA is not just diffusion- or swelling-controlled in either case (meaning that release is not only controlled by Fick diffusion and by matrix swelling) but is also largely influenced by the different ionic interactions that can be established between DXA, CS and [Ch][DHP].

CONCLUSIONS

The present work discussed the capacity of biocompatible ammonium-based ILs (choline chloride, [Ch][Cl], and choline dihydrogen phosphate, [Ch][DHP]) to work as modifiers for the stimuli responsiveness of chitosan. It was demonstrated that both ILs increased the conductivity and the actuation capacity of this natural polyelectrolyte when stimulated by a low electrical charge and that this effect is more evident for CS films loaded with [Ch][DHP]. Moreover, the conductivity was shown to increase with the amount of IL and to be dependent on the anion type and on the acidity of the medium. The medium acidity was particularly important for the conductivity of [Ch][DHP]-loaded films. This indicates that the mechanism of conduction of [Ch][DHP] loaded into CS films may result from a combination of the Grotthuss mechanism and a paddle wheel mechanism, similar to previously reported data for pure IL. The enhanced conductivity of [Ch][DHP], when compared to [Ch][Cl], is proposed to be due to the solid–solid phase transition characteristic of the former and that occurs around room temperature, as confirmed by DSC analysis. [Ch][DHP] also affected the release profile of dexamethasone sodium phosphate (DXA), which was systematically lower for IL-loaded chitosan films, independent of the pH of the release medium. Release results clearly indicated that the release of DXA is not just diffusion- or swelling-controlled, but it is also largely influenced by the different ionic interactions that can be established between DXA, CS, and [Ch][DHP]. Overall, the results obtained in this work lead to the conclusion that biocompatible and biodegradable ILs and polyelectrolytes can be conjugated to develop electrically and pH stimuli-responsive systems that can be further optimized to develop improved electrically modulated drug release systems for iontophoretic applications.

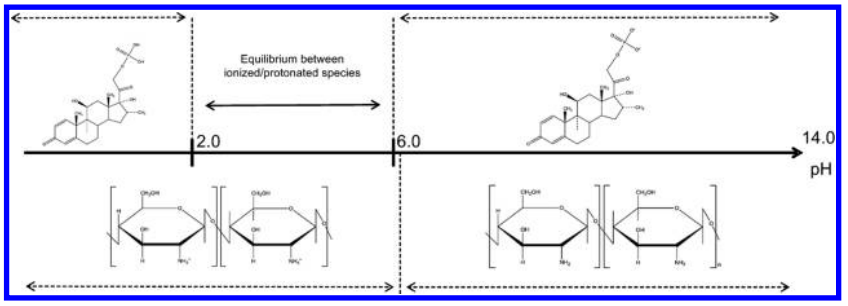

Figure 11. Identification of the ionic charges prevalence of DXA and CS chains (depending on the pH of the release media).

AUTHOR INFORMATION

Corresponding Authors

*Phone: +351-239-854470 (C.M.A.B.). Fax: +351-239-827703 (C.M.A.B.). E-mail address: cbrett@ci.uc.pt (C.M.A.B.).
*Phone: +351-239-798700 (H.C.d.S.). Fax: +351-239-798703 (H.C.d.S.). E-mail: hsousa@eq.uc.pt (H.C.d.S.).

Notes

The authors declare no competing financial interest.

ACKNOWLEDGMENTS

This work was financially supported by Fundação para a Ciência e Tecnologia (FCT-MEC) under contract PTDC/QUI/71398/2006 and PEst-C/EQB/UI0102/2011. A.M.A. Dias acknowledges FCT-MEC for the postdoctoral fellowship SFRH/BPD/40409/2007 and M.M.B. for the postdoctoral fellowship SFRH/BPD/72656/2010.

REFERENCES

(1) Tokarev, I.; Motornov, M.; Minko, S. Molecular-engineered stimuli-responsive thin polymer film: A platform for the development of integrated multifunctional intelligent materials. *J. Mater. Chem.* **2009**, *19*, 6932−6948.
(2) Holzapfel, B. M.; Reichert, J. C.; Schantz, J. T.; Gbureck, U.; Rackwitz, L.; Nöth, U.; Jakob, F.; Rudert, M.; Groll, J.; Hutmacher, D. W. How smart do biomaterials need to be? A translational science and clinical point of view. *Adv. Drug Delivery Rev.* **2012**, *65*, 581−603.
(3) Roy, D.; Cambre, J. N.; Sumerlin, B. S. Future perspectives and recent advances in stimuli-responsive materials. *Prog. Polym. Sci.* **2010**, *35*, 278−301.
(4) Perez, R. A.; Won, J. E.; Knowles, J. C.; Kim, H. W. Naturally and synthetic smart composite biomaterials for tissue regeneration. *Adv. Drug Delivery Rev.* **2012**, *65*, 471−496.
(5) Stuart, M. A.; Huck, W. T. S.; Genzer, J.; Müller, M.; Ober, C.; Stamm, M.; Sukhorukov, G. B.; Szleifer, I.; Tsukruk, V. V.; Urban, M.; Winnik, F.; Zauscher, S.; Luzinov, I.; Minko, S. Emerging applications of stimuli-responsive polymer materials. *Nat. Mater.* **2010**, *9*, 101−113.
(6) Murdan, S. Electro-responsive drug-delivery from hydrogels. *J. Controlled Release* **2003**, *92*, 1−17.
(7) Kost, J.; Langer, R. Responsive polymeric delivery systems. *Adv. Drug Delivery Rev.* **2001**, *46*, 125−148.
(8) Li, J.; Ma, W.; Song, L.; Niu, Z.; Cai, L.; Zeng, Q.; Zhang, X.; Dong, H.; Zhao, D.; Zhou, W.; Xie, S. Superfast-response and ultrahigh-power-density electromechanical actuators based on hierarchal carbon nanotube electrodes and chitosan. *ACS Nano* **2011**, *11*, 4636−4641.
(9) Liu, K. H.; Liu, T. Y.; Chen, S. Y.; Liu, D. M. Drug release behavior of chitosan−montmorillonite nanocomposite hydrogels following electrostimulation. *Acta Biomater.* **2008**, *4*, 1038−1045.
(10) Kumar, M. N. V. R.; Muzzarelli, R. A. A.; Muzzarelli, C.; Sashiwa, H.; Domb, A. J. Chitosan chemistry and pharmaceutical perspectives. *Chem. Rev.* **2004**, *104*, 6017−6084.
(11) Bhattarai, N.; Gunn, J.; Zhang, M. Chitosan-based hydrogels for controlled, localized drug delivery. *Adv. Drug Delivery Rev.* **2010**, *62*, 83−99.
(12) Croiser, F.; Jérôme, C. Chitosan-based biomaterials for tissue engineering. *Eur. Polym. J.* **2013**, *49*, 780−792.
(13) Sutani, K.; Kaetsu, I.; Uchida, K. The synthesis and the electric responsiveness of hydrogels entrapping natural polyelectrolyte. *Radiat. Phys. Chem.* **2001**, *61*, 49−54.
(14) Dong, S.; Li, Z.; Yu, Z.; Zhou, Y.; Tang, H. Direct electrochemistry of hemoglobin immobilized in chitosan-room temperature ionic liquid film and application in its interaction with 3,4-bis-(4-hydro-3-xycoumarin)-2,5-hexanediol. *Colloid Surf., B* **2012**, *100*, 133−137.
(15) Ma, B.; Li, X.; Qin, A.; He, C. A comparative study on the chitosan membranes prepared from glycine hydrochloride and acetic acid. *Carbohyd. Polym.* **2013**, *91*, 477−482.
(16) Silva, S. S.; Santos, T. C.; Cerqueira, M. T.; Marques, A. P.; Reys, L. L.; Silva, T. H.; Caridade, S. G.; Mano, J. F.; Reis, R. L. The use of ionic liquids in the processing of chitosan/silk hydrogels for biomedical applications. *J. Mater. Chem.* **2012**, *14*, 1463−1470.
(17) Stefanescu, C.; Dalya, W. H.; Negulescua, I. I. Biocomposite films prepared from ionic liquid solutions of chitosan and cellulose. *Carbohyd. Polym.* **2012**, *87*, 435−443.
(18) Dias, A. M. A.; Marceneiro, S.; Braga, M. E. M.; Coelho, J. F. J.; Ferreira, A. G. M.; Simões, P. N.; Veiga, I. M.; Tomé, L. C.; Marrucho, I. M.; Esperança, J. M. S. S.; Matias, A.; Duarte, C. M. M.; Rebelo, L. P. N.; de Sousa, H. C. Phosphonium-based ionic liquids as polymeric modifiers and their influence on the properties of biomedical grade poly(vinyl chloride). *Acta Biomater.* **2012**, *8*, 1366−1379.
(19) Zhang, Q.; Zhang, S.; Deng, Y. Recent advances in ionic liquid catalysis. *Green Chem.* **2011**, *13*, 2619−2637.
(20) Tang, B.; Bi, W.; Tian, M.; Row, K. H. Application of ionic liquid for extraction and separation of bioactive compounds from plants. *J. Chromatogr., B: Anal. Technol. Biomed. Life Sci.* **2012**, *904*, 1−21.
(21) Chen, C.; Yang, C. Preparation of cellulosic ion exchange fiber using an ionic liquid as reaction reagent and medium. *J. Appl. Polym. Sci.* **2011**, *122*, 2287−2294.
(22) Kubisa, P. Ionic liquids in the synthesis and modification of polymers. *J. Polym. Sci., Polym. Chem.* **2005**, *43*, 4676−4683.
(23) Armand, M.; Endres, F.; MacFarlane, D. R.; Ohno, H.; Scrosati, B. Ionic-liquid materials for the electrochemical challenges of the future. *Nat. Mater.* **2009**, *8*, 621−629.
(24) Prasad, K.; Kaneko, Y.; Kadokawa, J. Novel gelling of κ-,ι- and λ-carregeenans and their composite gels with cellulose using ionic liquid. *Macromol. Biosci.* **2009**, *9*, 376−382.
(25) Singh, P. K.; Bhattacharya, B.; Nagarale, R. K.; Kim, K.; Rhee, H. Synthesis, characterization and application of biopolymer-ionic liquid composite membranes. *Synth. Met.* **2010**, *160*, 139−142.
(26) Mecerreyes, D. Polymeric ionic liquids: Broadening the properties and applications of polyelectrolytes. *Prog. Polym. Sci.* **2011**, *36*, 1629−1648.
(27) Lu, W.; Fadeev, A. G.; Qi, B.; Smela, E.; Mattes, B. R.; Ding, J.; Spinks, G. M.; Mazurkiewicz, J.; Zhou, D.; Wallace, G. G.; MacFarlane,

D. R.; Forsyth, S. A.; Forsyth, M. Use of ionic liquids for pi-conjugated polymer electrochemical devices. *Science* **2002**, *297*, 983−987.
(28) Lin, J.; Liu, Y.; Zhang, Q. M. Charge dynamics and bending actuation in Aquivion membrane swelled with ionic liquids. *Polymer* **2011**, *52*, 540−546.
(29) Xiong, Y.; Wang, H.; Wu, C.; Wang, R. Preparation and characterization of conductive chitosan-ionic liquid composite membranes. *Polym. Adv. Technol.* **2012**, *23*, 1429−1434.
(30) Yamagata, M.; Soeda, K.; Ikebe, S.; Yamazaki, S.; Ishikawa, M. Chitosan-based gel electrolyte containing an ionic liquid for high-performance nanoqueous supercapacitors. *Electrochim. Acta* **2012**, *100*, 275−280.
(31) Petkovic, M.; Ferguson, J. L.; Gunaratne, H. Q. N.; Ferreira, R.; Leitão, M. C.; Seddon, K. R.; Rebelo, L. P. N.; Pereira, C. S. Novel biocompatible cholinium-based ionic liquids − Toxicity and biodegradability. *Green Chem.* **2010**, *10*, 643−649.
(32) Pernak, J.; Chwala, P. Synthesis and anti-microbial activities of choline-like quaternary ammonium chlorides. *Eur. J. Med. Chem.* **2003**, *38*, 1035−1042.
(33) Brock, M.; Nickel, A. C.; Madziar, B.; Blusztajn, J. K.; Berse, B. Differential regulation of the high affinity choline transporter and the cholinergic locus by cAMP signaling pathways. *Brain Res.* **2007**, *1145*, 1−10.
(34) Egashira, M.; Okada, S.; Yamaki, J.; Yoshimoto, N.; Morita, M. Effect of small cation addition on the conductivity of quaternary ammonium ionic liquids. *Electrochim. Acta* **2005**, *50*, 3708−3712.
(35) Vijayaraghavan, R.; Thompson, B. C.; MacFarlane, D. R.; Kumar, R.; Surianarayanan, M.; Aishwarya, S.; Sehgal, P. K. Biocompatibility of choline salts as crosslinking agents for collagen based biomaterials. *Chem. Commun.* **2010**, *46*, 294−296.
(36) OECD SIDS. Screening information Data Set (SIDS) for High Production Volume Chemicals. IPCSIN CHEM, 2004. http://www.inchem.org/documents/sids/sids/67481.pdf (accessed February 27, 2012).
(37) Weaver, K. D.; Kim, H. J.; Sun, J.; MacFarlane, D. R.; Elliott, G. D. Cyto-toxicity and biocompatibility of a family of choline phosphate ionic liquids designed for pharmaceutical applications. *Green Chem.* **2010**, *12*, 507−513.
(38) Weaver, K. D.; Vrikkis, R. M.; Van Vorst, M. P.; Trullinger, J.; Vijayaraghavan, R.; Foureau, D. M.; McKillop, I. H.; MacFarlane, D. R.; Krueger, J. K.; Elliott, G. D. Structure and function of proteins in hydrated choline dihydrogen phosphate ionic liquid. *Phys. Chem. Chem. Phys.* **2012**, *14*, 790−801.
(39) MacFarlane, D. R.; Forsyth, M. Plastic crystal electrolyte materials: New perspectives on solid state ionics. *Adv. Mater.* **2001**, *12*−*13*, 957−966.
(40) Yoshizawa-Fujita, M.; Fujita, K.; Forsyth, M.; MacFarlane, D. R. A new class of proton-conducting ionic plastic crystals based on organic cations and dihydrogen phosphate. *Electrochem. Commun.* **2007**, *9*, 1202−1205.
(41) Rana, U. A.; Bayley, P. M.; Vijayaraghavan, R.; Howlett, P.; MacFarlane, D. R.; Forsytha, M. Proton transport in choline dihydrogen phosphate/H_3PO_4 mixtures. *Phys. Chem. Chem. Phys.* **2010**, *12*, 11291−11298.
(42) Wan, Y.; Creber, K. A. M.; Peppley, B.; Bui, V. T. Synthesis, characterization and ionic conductive properties of phosphorylated chitosan membranes. *Macromol. Chem. Phys.* **2003**, *204*, 850−858.
(43) Wiles, J. L.; Vergano, P. J.; Barron, F. H.; Bunn, J. M.; Testin, R. F. Water vapor transmission rates and sorption behavior of chitosan films. *J. Food Sci.* **2000**, *65*, 1175−1179.
(44) Mano, J. F. Viscoelastic properties of chitosan with different hydration degrees as studied by dynamic mechanical analysis. *Macromol. Biosci.* **2008**, *8*, 69−76.
(45) Pereda, M.; Aranguren, M. I.; Marcovich, N. E. Water vapor absorption and permeability of films based on chitosan and sodium caseinate. *J. Appl. Polym. Sci.* **2009**, *111*, 2777−2784.
(46) Oliver, L.; Meinders, M. B. J. Dynamic water vapour sorption in gluten and starch films. *J. Cereal Sci.* **2011**, *54*, 409−412.
(47) Kolodziejska, I.; Piotrowska, B. The water vapour permeability, mechanical properties and solubility of fish gelatin−chitosan films modified with transglutaminase or 1-ethyl-3-(3-dimethylaminopropyl) carbodiimide (EDC) and plasticized with glycerol. *Food Chem.* **2007**, *103*, 295−300.
(48) Moura, C. M.; Moura, J. M.; Santos, J. P.; Kosinski, R. C.; Dotto, G. L.; de Almeida Pinto, L. A. Evaluation of mechanical properties and water vapor permeability in chitosan biofilms using sorbitol and glycerol. *Macromol. Symp.* **2012**, *319*, 240−245.
(49) Suyatma, N. E.; Tighzert, L.; Copinet, A. Effects of hydrophilic plasticizers on mechanical, thermal and surface properties of chitosan films. *J. Agric. Food Chem.* **2005**, *53*, 3950−3957.
(50) Prasad, K.; Mine, S.; Kaneko, Y.; Kadokawa, J. Preparation of cellulose-based ionic porous material compatibilized with polymeric ionic liquid. *Polym. Bul.* **2010**, *64*, 341−349.
(51) Ma, B.; Zhang, M.; He, C.; Sun, J. New binary ionic liquid system for the preparation of chitosan/cellulose composite fibers. *Carbohyd. Polym.* **2012**, *88*, 347−351.
(52) Barsoukov, E.; Macdonald, J. R., Eds.; *Impedance Spectroscopy. Theory Experiment and Applications*, 2nd ed.; Wiley, New York, 2005.
(53) Barsan, M. M.; Pinto, E. M.; Florescu, M.; Brett, C. M. A. Development and characterization of a new conducting carbon composite electrode. *Anal. Chim. Acta* **2009**, *635*, 71−78.
(54) Lopez-Chavez, E.; Martinez-Magadan, J. M.; Oviedo-Roa, R.; Guzman, J.; Ramirez-Salgado, J.; Marin-Cruz, J. Molecular modeling and simulation of ion-conductivity in chitosan membranes. *Polymer* **2005**, *46*, 7519−7527.
(55) Ramirez-Salgado, J. Study of basic biopolymer as proton membrane for fuel cell systems. *Electrochim. Acta* **2007**, *52*, 3766−3778.
(56) Srinophakun, T.; Martkumchan, S. Ionic conductivity in a chitosan membrane for a PEM fuel cell using molecular dynamics simulation. *Carbohyd. Polym.* **2012**, *88*, 194−200.
(57) Ueki, T.; Watanabe, M. Macromolecules in ionic liquids: Progress, challenges, and opportunities. *Macromolecules* **2008**, *11*, 3739−3749.
(58) Yamada, M.; Honma, I. Anhydrous proton conductive membrane consisting of chitosan. *Electrochim. Acta* **2005**, *50*, 2837−2841.
(59) Rana, U. A.; Forsyth, M.; MacFarlane, D. R.; Pringle, J. M. Toward protic ionic liquid and organic ionic plastic crystal electrolytes for fuel cells. *Electrochim. Acta* **2012**, *84*, 213−222.
(60) Chahil, L. S.; Rana, U. A.; Forsyth, M.; Smith, M. E. Investigation of proton dynamics and the proton transport pathway in choline dihydrogen phosphate using solid-state NMR. *Phys. Chem. Chem. Phys.* **2010**, *12*, 5431−5438.
(61) Rana, U. A.; Vijayaraghavan, R.; MacFarlane, D. R.; Forsyth, M. Plastic crystal phases with high proton conductivity. *J. Mater. Chem.* **2012**, *22*, 2965−2974.
(62) Lu, L.; Chen, W. Biocompatible compoiste actuator: a supramolecular structure consisting of the biopolymer chitosan, carbon nanotubes, and an ionic liquid. *Adv. Mater.* **2010**, *22*, 3745−3748.
(63) Wang, N.; Chen, Y.; Kim, J. Electroactive paper actuator made with chitosan-cellulose films: effect of acetic acid. *Macromol. Mater. Eng.* **2007**, *292*, 748−753.
(64) Berger, J.; Reist, M.; Mayer, J. M.; Felt, O.; Peppas, N. A.; Gurny, R. Structure and interactions in covalently and ionically crosslinked chitosan hydrogels for biomedical applications. *Eur. J. Pharm. Biopharm.* **2004**, *57*, 19−34.
(65) Cázares-Delgadillo, J.; Balaguer-Fernández, C.; Calatayud-Pascual, A.; Ganem-Rondero, A.; Quintanar-Guerrero, D.; López-Castellano, A. C.; Merino, V.; Kalia, Y. N. Transdermal iontophoresis of dexamethasone sodium phosphate in vitro and in vivo: Effect of experimental parameters and skin type on drug stability and transport kinetics. *Eur. J. Pharm. Biopharm.* **2010**, *75*, 173−178.
(66) Spinks, G. M.; Lee, C. H.; Wallace, G. G.; Kim, S. I.; Kim, S. J. Swelling behavior of chitosan hydrogels in ionic liquid-water binary systems. *Langmuir* **2006**, *22*, 9375−9379.

(67) Bhumkar, D. R.; Pokharkar, V. B. Studies of effect on pH on cross-linking of chitosan with sodium tripolyphosphate: A technical note. *AAPS Pharm. Sci. Technol.* **2006**, *7*, E1−E6.